

---

# Metabolic Cardiac Imaging in Severe Coronary Disease: Assessment of Viability with Iodine-123-Iodophenylpentadecanoic Acid and Multicrystal Gamma Camera, and Correlation with Biopsy

Gary Murray, Nikolaus Schad, William Ladd, David Allie, Roger Vander Zwagg, Phillip Avet, and John Rockett

*Cardiovascular Institute of the South, Houma, Louisiana; Institute of Radiological and Imaging Sciences, University of Siena, Italy; Health Services Research and Nuclear Medicine Department, Baptist Memorial Hospital, Memphis, Tennessee; and Terrebonne General Medical Center, Houma, Louisiana*

---

Fifteen patients with coronary disease and resting left ventricular ejection fractions of  $\leq 0.35$  underwent resting metabolic cardiac imaging utilizing 1 mCi [ $^{123}\text{I}$ ]iodophenylpentadecanoic acid (IPPA) intravenously and a multicrystal gamma camera. Parametric images of regional rates of IPPA clearance and accumulation were generated. Forty-two vascular territories (22 infarcted) were evaluated by metabolic imaging as well as transmural myocardial biopsy. Despite resting akinesis or dyskinesis in 20/22 (91%) infarcted territories, 16/22 (73%) of these territories were metabolically viable. Transmural myocardial biopsies in all patients (43 sites, 42 vascular territories) during coronary bypass surgery confirmed IPPA results in 39/43 patients (91%). When compared to biopsy, scan sensitivity for viability was 33/36 (92%) with a specificity of 6/7 (86%). Eighty percent of bypassed, infarcted but IPPA viable segments demonstrated improved regional systolic wall motion postoperatively as assessed by exercise radionuclide angiography. We conclude resting IPPA imaging identifies viable myocardium, thereby providing a safe, cost-effective technique for myocardial viability assessment.

**J Nucl Med 1992; 33:1269-1277**

---

**M**ycocardial revascularization has created the necessity for reliable differentiation of viable, stunned (1,2) or hibernating (3) myocardium from irreversibly damaged tissue. Over one million Americans experience a myocardial infarction each year (4). Many are candidates for thrombolysis (5,6), emergent or delayed angioplasty (7) or bypass graft surgery (8,9). A rapid, reliable, safe and cost-effective method of determining the presence of viable myocardium within the infarction zone should profoundly impact decisions regarding these revascularization procedures.

---

Received Aug. 12, 1991; revision accepted Mar. 10, 1992.  
For reprints contact: Gary L. Murray, MD, Suite 210, 5220 Park Ave., Memphis, TN 38119.

Wall motion analysis, unfortunately, cannot accomplish this if a severe wall motion abnormality is present (10). PET scanning (11), MRI (12) and echocardiographic analysis of backscatter (13,14) have been utilized successfully for evaluation of myocardial viability. PET's great disadvantage is its cost. Furthermore, like MRI, it is not easily accomplished in acutely ill, unstable patients. Currently, transthoracic interrogation of the myocardium for backscatter analysis is subject to the limitations of body habitus, as is standard echocardiography.

However, [ $^{123}\text{I}$ ]iodophenylpentadecanoic acid (IPPA), a fatty acid that has demonstrated promise in assessing myocardial viability (15), can be imaged with a standard single crystal (15-20) or multicrystal (21,22) gamma camera. Furthermore, because of a 13-hr half-life, an onsite cyclotron is not required. Therefore, IPPA imaging has the potential of being a cost-effective, commonly available alternative to the other techniques.

## METHODS

Fifteen subjects with coronary artery disease and resting left ventricular ejection fractions (LVEFs)  $< 0.35$  (Table 1), stable enough for at least low-level exercise testing, underwent two-dimensional echocardiography, cardiac catheterization, RNA exercise and resting IPPA imaging. Two-dimensional echocardiography was performed on a Hewlett Packard Sonos 500, with regional wall motion qualitatively graded as normal, hypokinetic, akinetic or dyskinetic. Regional wall motion was similarly qualitatively evaluated by cineangiographic left ventriculography. When the circumflex was an infarct-related vessel, biplane cineangiography of the left ventricle was accomplished. Radionuclide angiography (RNA) testing was accomplished utilizing previously described techniques (23) and the Baird System 77.

Metabolic imaging was also accomplished as previously described (21,22). One millicurie IPPA (MYOPURE<sup>®</sup>, provided by Nordion International Inc., with quality control by Syncor<sup>®</sup>) was injected as a bolus through an antecubital fossa vein at rest. All patients were imaged under fasting conditions, lying or sitting before an multicrystal detector (Baird System 77) in the anterior

**TABLE 1**  
Patient Characteristics

Total subjects	15
Demographics	
Mean age	61 yr
Male	87%
Female	13%
VEF	
Mean at rest	31%
Mean during exercise	32%
MI culprit vessel*	
LAD	23%
CFX	36%
RCA	41%
MI wall motion abnormality	
Akinesis	82%
Dyskinesis	9%
Severe hypokinesis	9%
Number of vessels with stenosis	≥50%
1	7%
2	20%
3	73%

\* Seven patients had experienced two MIs by different vessels.

view. Six drops of potassium iodide (SSKI, 1 g/ml) were given orally prior to IPPA administration in order to block thyroid uptake of the isotope. A total of 1500 frames were acquired over 25 min at 1 frame/sec. Since IPPA is injected as a small bolus, imaging at 1 frame/sec allows the generation of an initial histogram over the heart area, displaying sequentially the right ventricular peak, the left ventricular peak (first-pass) and a third maximum representing myocardial uptake. The curve between the second and third peaks therefore reflects left ventricular cavity washout and myocardial washin (uptake); the washout being a function of LVEF (recirculation excluded) and the left ventricular washin a function of left ventricular washout and resistance to inflow. To define the heart mask, a region of interest (ROI) of the first-pass LV activity is extended to the ventricular border on an image derived from the initial phase of LV uptake. Edge detection is accomplished by spatial gradients (24,25). This heart mask is then checked on both an original initial and end-phase of acquisition image in order to correct for any hepatic overlap.

After regrouping the heart data to 4 frames/min, ROIs of the anterior, inferior and basal LV walls are selected and time-activity curves are generated. The course of the LV first-pass washout and myocardial washin allows individual selection of the appropriate initial time interval for the computation of regional rates of metabolism.

The regrouped 100 images are divided by the heart mask and the regional rates of activity, decreasing (reflecting beta oxidation) or increasing (reflecting accumulation) (21,22), are computed for each pixel for different time intervals using the least squares fit regression method (26,27). This generates two numerical matrices displayed as color-coded parametric images, one of the rate of decreasing activity, and one of the rate of increasing activity. The two parametric images are processed for the following intervals:

1. Predominant perfusion uptake phase, 45 sec to 2.5–3 min postinjection.
2. Early metabolic phase, 3–10 min.

3. Mid-metabolic phase, 10–17 min.
4. Late metabolic phase, 17–24 min.

The parametric images represent average regional rates for these time intervals. During metabolism, the decrease image shows the regional slopes of metabolic clearing rates (beta oxidation), and the increase image displays zones where IPPA is esterified to triblyceride and phospholipids (21,22). Finally, the sum of the decrease and increase images (3–24 min) is generated so that regions without any or with low metabolic activity can be identified easily. To avoid the problem of IPPA storage as phospholipid/triglyceride affecting IPPA washout, the 3–24-min summed increase (accumulation) image was inspected for evidence of storage. Nonviability required no significant storage of IPPA within the ROI, since accumulation can occur in viable, ischemic myocardium when fatty acid esterification to triglycerides exceeds lipolysis (28).

Infarcted vascular territories were chosen for evaluation as follows:

1. If Q-waves ± chronic ST-segment elevation were present in electrocardiographic leads II, III, AVF, the right coronary artery (RCA) [or if dominant, the circumflex (CFX)] was evaluated for viability; if these same electrocardiographic changes were present V1–V6, the left anterior descending (LAD) was assessed. Tall, broad R-waves in V1 and V2 in the absence of inferior Q's were used to indicate prior circumflex infarction, unless the circumflex was dominant. The electrocardiographic findings were correlated with cardiac catheterization and echocardiographic wall motion to avoid electrocardiographic pseudo-infarction patterns.
2. If there was no electrocardiographic evidence of prior infarction, then the vessel supplying an akinetic/dyskinetic LV wall at cardiac catheterization was evaluated. From one to three vascular territories were evaluated per patient. Once identified as an infarcted territory by electrocardiogram, two-dimensional echocardiographic and cardiac catheterization findings, the territory to be evaluated for viability was assigned a location on the RNA and IPPA scans (Fig. 1).

Myocardial viability was determined as follows:

- 1a. IPPA washout was viable when at least 50% of the LV area supplied by the chosen vessel demonstrated at least 16% elimination of IPPA. Seventeen healthy volunteers with normal two-dimensional echocardiograms and no RNA exercise evidence of infarction or ischemia underwent resting IPPA imaging. All volunteers were less than 40 yr old. Three to 25-min segmental IPPA washout rates were calculated from the time-activity curves to overcome the problem of varying input into the myocardium. After 3 min, the blood-pool activity is low (for example, the aorta is no longer visible), and this small amount of blood-pool activity, in comparison to the high myocardial values, should not greatly influence the rate images (first derivative of the time-activity curve). Mean washout was  $21.2\% \pm 5.0\%$ . Therefore, at least 16% IPPA washout (mean washout – 1 s.d.) in the segments supplied by the infarction-related artery was required for metabolic viability. Since, for example, a LAD-related infarction could demonstrate nonviability apically as well as viability anterolaterally and

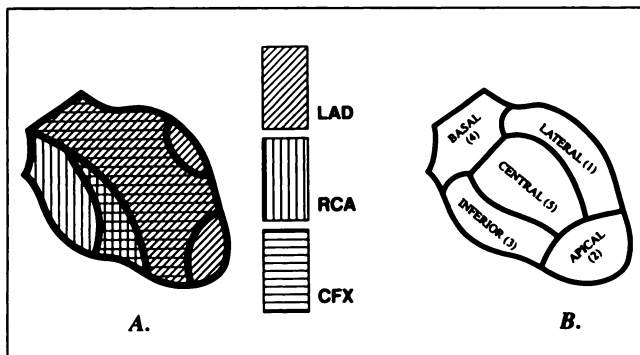


**FIGURE 1.** Assignment of left ventricular regions into vascular territories (A) and segments (B). Therefore, an apical defect would be assigned to the LAD and an inferobasal defect to the RCA. A homogeneous defect involving lateral, central, and inferior segments would be designated CFX-related.

in the septum, normal washout was required to be present in at least 50% of the LV area supplied by the infarct-related vessel. It was felt that viability in at least 50% of the infarcted segment should represent a clinically reasonable criterion to consider revascularization, either with bypass surgery or angioplasty. The percent of the left ventricular area over which IPPA washout was calculated was easily determined by the number of pixels in the ROI, in comparison to the total number of pixels over the entire left ventricle, both being displayed on screen by the program. So, determination of myocardial viability sufficient for a revascularization procedure relied on the degree and extent of regional IPPA clearing in the coronary vascular territory. Washout was calculated as follows: (3-min cts – 25-min cts) ÷ 3-min cts.

- 1b. If IPPA washout was 15% or less, the segment was considered nonviable unless appreciable IPPA storage (accumulation) was noted within at least 50% of the segment's area.
2. Biopsy was viable if standard hematoxylin and eosin, as well as trichrome, stains demonstrated less than 50% replacement fibrosis within the transmural biopsy. Biopsies were interpreted by an independent pathologist (PA). Only one subject was biopsied within 1 mo of infarction, and the involved territory was mostly viable with well-preserved myocytes and only a small area of loss of myocyte nuclei, striations, and development of myocyte granularity.

Sensitivity and specificity for viability were defined as follows:

$$\text{sensitivity} = \frac{\text{segments biopsy and IPPA viable}}{\text{segments biopsy viable}};$$

$$\text{specificity} = \frac{\text{segments biopsy and IPPA nonviable}}{\text{segments biopsy nonviable}}$$

The data were analyzed using standard statistical techniques for categorical variables. Vascular territories of the heart, both within the same patient as well as among different patients, were considered independent experimental units. Proportions within independent subgroups of patients, or territories of the heart, were compared using chi-square analysis for contingency tables.

## RESULTS

### Resting IPPA Viability Assessment

The characteristics of the study population are presented in Table 1. Forty-two vascular territories (14 LAD, 14 circumflex, 14 RCA) were evaluated. Nine of 14 (64%) CFX territories were metabolically viable, in comparison to 13/14 (93%) RCA and 11/14 (79%) LAD distributions ( $p = \text{ns}$ ). Of the 22 infarcted territories, 20/22 (91%) were akinetic or dyskinetic, and 16/22 (73%) were metabolically viable: 4/5 (80%) LAD, 5/8 (63%) circumflex, and 8/9 (89%) right coronary ( $p = \text{ns}$ ).

### Correlation of Resting IPPA Scans with Transmural Myocardial Biopsies

Fifteen patients were biopsied at 43 myocardial sites (42 vascular territories). Replacement fibrosis involving at least 50% of the biopsy (hematoxylin and eosin as well as trichrome stain) was considered evidence of nonviability. Biopsies correlated well with IPPA results, with 33 sites viable by both techniques (11 LAD, 10 CFX, 12 right coronary) and 6 sites nonviable by both (Fig. 2). Therefore, in 39/43 (91%), the biopsy and IPPA results were concordant; of the three discordant biopsies, two biopsies were viable (one LAD, one CFX) and one nonviable (LAD). The 3–25-min IPPA clearance in biopsy viable segments was  $17.8\% \pm 2.3\%$  compared to  $21.2\% \pm 5.0\%$  IPPA washout in the healthy volunteers ( $p = 0.016$ ), and  $13.4\% \pm 2.4\%$  clearance in biopsy nonviable segments ( $p < 0.001$  versus biopsy viable segments;  $p < 0.0001$  versus healthy volunteers). By utilizing biopsy viability as the gold standard, the sensitivity of resting IPPA for viability was 33/36 (92%), with the specificity being 6/7 (86%).

### Preoperative Versus Postoperative RNA Wall Motion

Following coronary bypass surgery, systolic regional wall motion, resting and/or exercise, improved in 12/16 (75%) infarcted and IPPA viable segments and did not improve in 4/6 (67%) infarcted, IPPA nonviable segments. One infarcted, IPPA viable segment was not revascularized. Therefore, 12/15 (80%) infarcted, IPPA viable, revascularized segments demonstrated improved systolic regional wall motion postoperatively, either at rest and/or during exercise.

Although systolic regional wall motion improved in 80% of revascularized, viable segments postoperatively, global LVEF increased only in the three patients with prior anterior infarctions but IPPA and biopsy viable LAD territory, with a mean resting LVEF increasing from  $0.32 \pm 0.04$  to  $0.39 \pm 0.17$  ( $p = \text{ns}$ ) and a mean exercise LVEF increasing from  $0.28 \pm 0.07$  to  $0.43 \pm 0.14$  ( $p = 0.001$ ). Bypassed patients with nonviable LAD territories showed no trend for improvement in LVEF.

The following four cases are illustrative.

Case 1: A 28-yr-old female healthy volunteer (Fig. 3).

Case 2 (Fig. 4A): 68-yr-old female whose IPPA scan 10 days postanterior myocardial infarction with anterior aki-

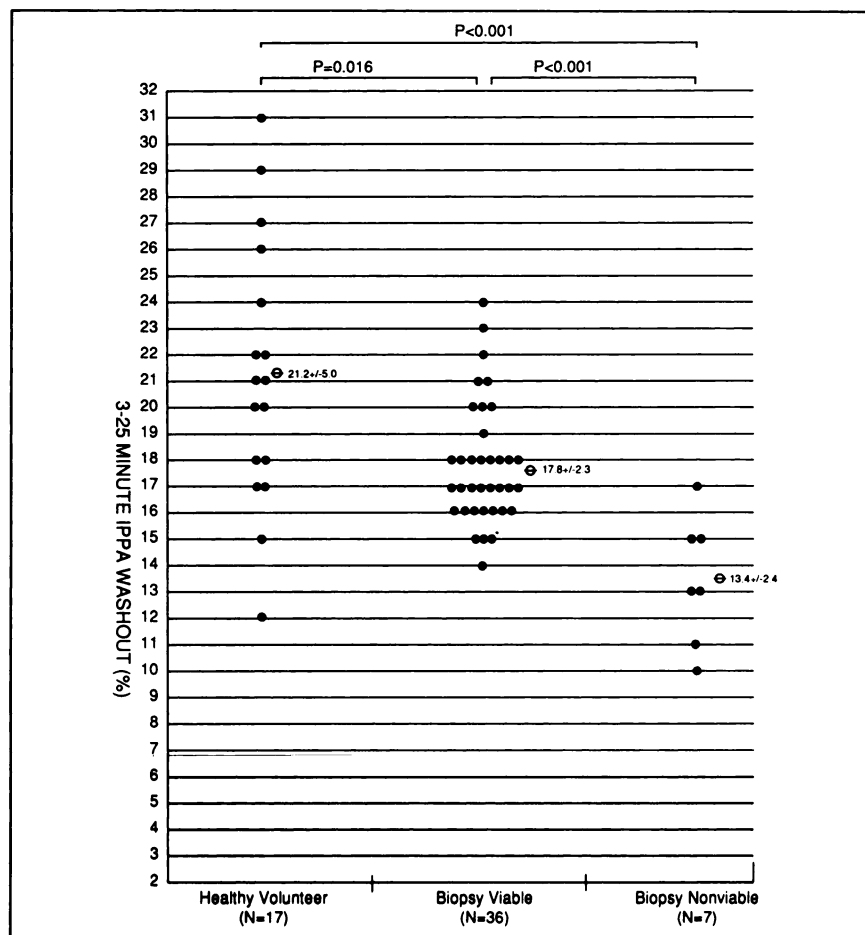


**FIGURE 2.** Three- to 25-min IPPA myocardial washout in healthy volunteers and patients with viable as well as nonviable transmural myocardial biopsies. \* This vascular territory demonstrated accumulation of IPPA.

nesis revealed a 3–25-min IPPA washout from the LAD distribution (32% of LV pixels) of 17%. Only 5% of the LV pixels had  $\leq 15\%$  washout.

Case 3 (Fig. 4B): 47-yr-old male whose IPPA scan following remote anterior and inferior myocardial infarctions demonstrated 18% washout from the RCA distribution (18% of LV pixels). Pixels with  $\leq 15\%$  washout are located primarily within the LAD territory (13% of LV pixels).

Case 4 (Fig. 4C): 77-yr-old male whose IPPA scan following a remote posterolateral myocardial infarction showed 16% washout from the most abnormal area of the circumflex distribution (7% of LV pixels).

## DISCUSSION

### Suitability of IPPA for Metabolic Imaging

IPPA has been proven to parallel  $^{14}\text{C}$ -palmitate in its metabolism (29). At rest, its myocardial uptake is directly proportional to myocardial blood flow up to 150 cc/min/100 g (30). It crosses the sarcolemma by facilitated diffusion, and, in the presence of adequate oxygenation, is activated by coenzyme A, transferred by carnitine into the mitochondria and rapidly beta oxidized (half-time 11 min) to iodobenzoic acid, producing adenosine triphosphate

(31). A portion of IPPA is metabolized more slowly (half-time 76 min), reflecting that fraction of the IPPA that has been incorporated into phospholipid and triglyceride pools and subsequently also metabolized. Therefore, IPPA myocardial elimination is biexponential. Unlike heptadecanoic acid, there is no significant iodine dissociation from IPPA during metabolism (29). Fatty acid uptake and beta oxidation are reduced during ischemia (32). This reduction in beta oxidation can even result in transient accumulation of fatty acid as triglyceride (28).

Iodine-123 is a relatively high-energy gamma emitter, with a 159 keV and possesses a 13-hr shelf half-life. Consequently, IPPA is ideal for imaging with a single- or multicrystal gamma camera and does not require an onsite cyclotron.

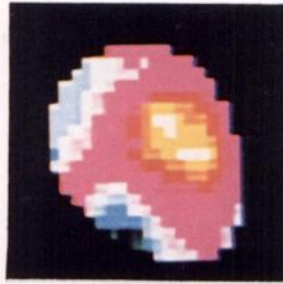
IPPA has been evaluated extensively utilizing a single-crystal camera to create planar and tomographic images of left ventricular metabolism (15–20). Typically for tomography, 6–8 mCi of IPPA are injected intravenously, and the imaging time is approximately 54 min. Insofar as diagnosing exercise-induced ischemia, IPPA has been found to be at least comparable to thallium (19,20). IPPA uptake in irreversibly damaged myocardium is severely reduced to approximately 6% of normal areas (33). IPPA clearance in infarcted areas is significantly impaired com-

Early IPPA Elimination  
Rate Image (3-10 min.)



A

Mid IPPA Elimination  
Rate Image (10-17 min.)



B

Late IPPA Elimination  
Rate Image (17-24 min.)



C

Summed IPPA Elimination  
Rate Image (3-24 min.)



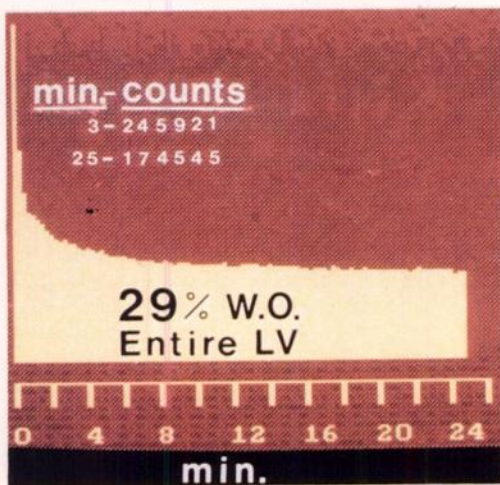
D<sub>1</sub>

Summed IPPA Elimination Rate Image  
with ROI (3-24 min.)



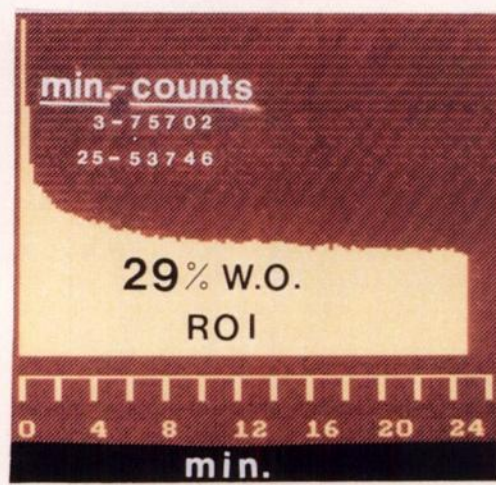
D<sub>2</sub>

IPPA Time Activity Curve  
Entire L.V. (3-25 min.)



E

IPPA Time Activity Curve  
with ROI (3-25 min.)



F

**FIGURE 3.** Case 1: A 28-yr-old healthy volunteer. (A) Early metabolic IPPA image (3–10 min) reveals prompt, vigorous symmetric elimination of the radioisotope. (B) Mid-metabolic image (10–17 min). (C) Late metabolic image (17–24 min). (D1) Summed metabolic image (3–24 min). (D2) ROI chosen for washout analysis shown as black pentagon. (E) Time-activity (washout) curve from the entire left ventricle. (F) Time-activity curve from the ROI. Both (E) and (F) demonstrate normal IPPA washout, with the fastest washout yellow and the slowest washout blue. WO = washout of IPPA.

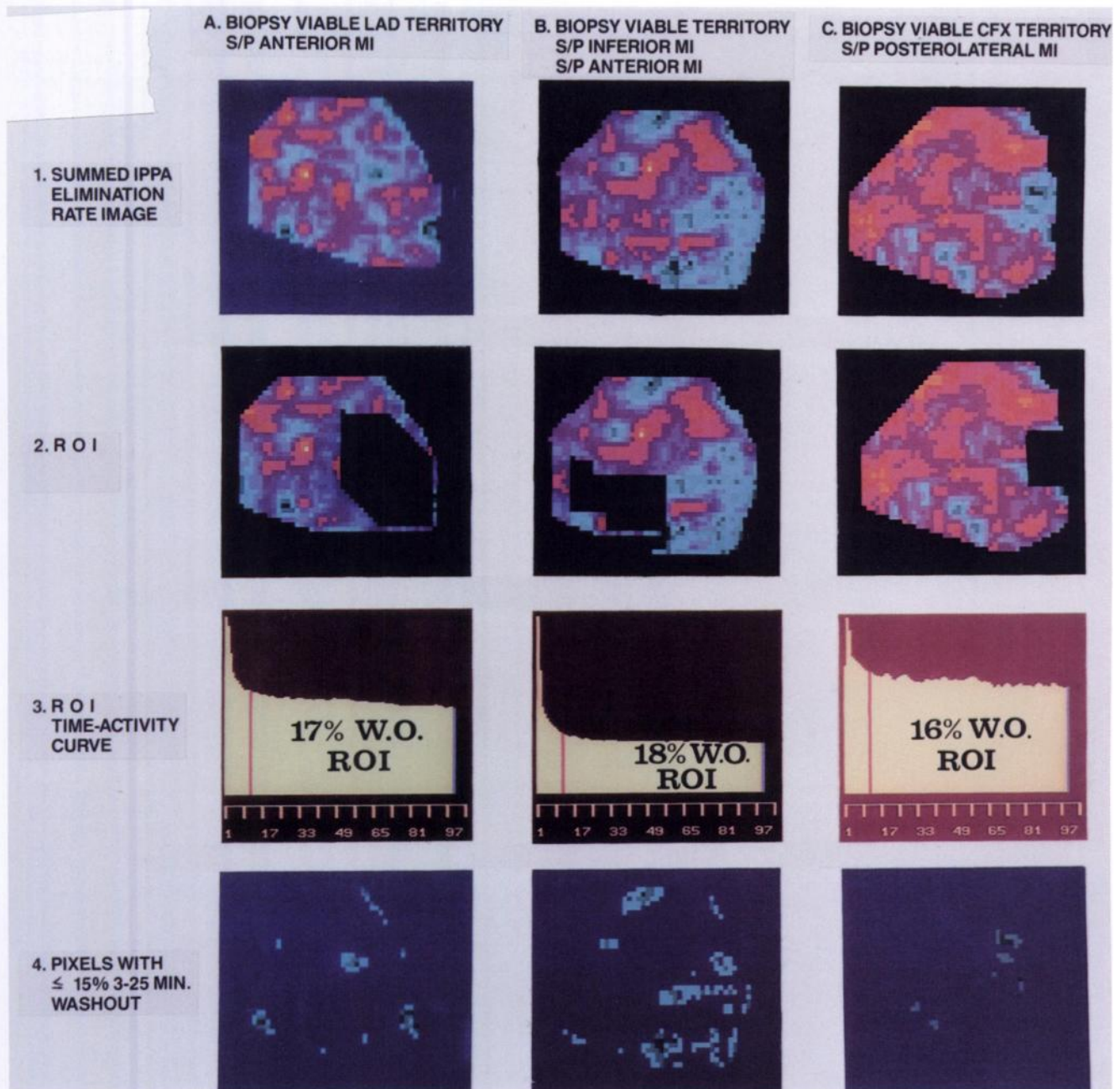


**FIGURE 4.** (A) Case 2: Anterior infarction (akinesis) with viability. The ROI covers most of the LAD's area, represents 32% of left ventricular pixels and has 17% 3–25-min IPPA washout. Only 66/1245 (5%) of the pixels have  $\leq 15\%$  washout. (B) Case 3: Inferior infarction (akinesis) with viability; also anteroapical infarction (akinesis). The ROI covers most of the RCA's area, represents 18% of left ventricular pixels and has 18% 3–25-min washout, with 187/1443 (13%) of the pixels having  $\leq 15\%$  washout, located mostly anteroapically. (C) Case 4: Posterolateral infarction (akinesis) with viability. The ROI covers a moderate area and 95/1450 (7%) of the pixels represent the slowest washout within a portion of the circumflex territory and has 16% 3–25-min washout with accumulation. WO = washout of IPPA.

pared to washout in normal myocardium (34,35). Therefore, we anticipated finding reduced IPPA clearance of nonviable segments in our subjects.

There is much less experience with imaging IPPA using a multicrystal camera (21,22). The 3–25-min IPPA clearing rate of  $21.2\% \pm 5.0\%$  in our normal volunteers is less than the normal 5–25-min washout of approximately 40%

in dogs utilizing tomograms obtained with a single-crystal gamma camera (36). However, our clearing rate is similar to the 4–20-min washout of  $21.1\% \pm 10\%$  in normal human volunteers imaged with a single crystal planar technique (18). The multicrystal technique provides the advantages of lowering the cost of the study since only 1 mCi IPPA is required (instead of 6–8 mCi with the single-

crystal technique), reduction of imaging time by 50% compared to tomographic techniques (excluding the triple-head camera) and portability of some of the newer multicrystal systems.

### Results of the Present Study

Seventy-three percent of infarcted territories were metabolically viable. Biopsy nonviable segments had lower IPPA clearance than biopsy viable segments:  $13.4\% \pm 2.4\%$  versus  $17.8\% \pm 2.3\%$  ( $p < 0.001$ ) (Fig. 2). Our IPPA clearance in nonviable segments is greater than the clearance of  $6.3\% \pm 3.8\%$  found in a previous study of patients with prior myocardial infarction utilizing planar imaging (35). All of our patients had angiographic collateral vessels supplying the infarcted territories. Since collaterals affect IPPA kinetics (37), perhaps collateralization (and possibly overlapping viable segments) increased apparent washout in nonviable areas and likely contributed to our high viability in infarcted segments. Previous studies utilizing fluorodeoxyglucose found 16/32 (50%) acutely infarcted territories viable (38) and 54% of chronic Q-wave infarctions viable (39).

The  $17.8\% \pm 2.3\%$  3–25-min IPPA clearance from biopsy viable segments was significantly less than the  $21.2\% \pm 5.0\%$  clearance in healthy volunteers ( $p = 0.016$ ). This is not entirely unexpected, since viable biopsies were allowed to contain up to 50% fibrosis. Furthermore, 93% of subjects had multivessel disease, and it is therefore possible that some viable segments were ischemic.

This study utilizes transmural LV biopsies obtained during coronary bypass graft surgery as the gold standard for human myocardial viability. With this standard, IPPA sensitivity was 92% with a specificity of 86%.

Although not statistically significant with our sample size, the RCA territory tended to display the highest infarcted-segment metabolic viability, 8/9 (89%), despite imaging in only the anterior view. The RCA distribution may have superior collateral flow (40), and this may partly account for this observation. Conversely, the CFX distribution reflected the lowest infarction viability, 5/8 (63%).

In studies with fluorodeoxyglucose, 85% of viable segments improved resting wall motion following revascularization (11). In our study, 12/15 (80%) of IPPA viable segments bypassed, and only 2/6 (33%) of IPPA nonviable segments demonstrated improved postoperative regional wall motion. Resting IPPA imaging correctly predicted the postoperative regional wall motion response in 76% of infarcted segments.

### Limitations

SPECT IPPA studies provide multiple views, as opposed to a single-view utilizing our multicrystal camera planar technique. Obviously, overlap of vascular territories is a potential problem. However, the shape and location of the defects, especially peripheral defects apically and infero-

basally where overlap is minimal, allowed precise identification of the vascular territory involved (Fig. 1). Furthermore, the imaging view can be altered if desired (for example, imaging in the left lateral projection when the circumflex is being evaluated). The LAD, clinically the most important territory, forms the anterior cardiac border in the adopted anterior view and poses no problem in analysis with our technique. Planar imaging allows an accurate dynamic analysis of the course of regional metabolic events because of the high acquisition rate (1 image/sec) and the distinction between zones with predominant clearing and predominant accumulation of IPPA. Moreover, the lower isotope cost of our technique (one-sixth to one-eighth less than tomographic IPPA), the rapid identification of myocardial viability (by 10 min in 74% of patients and 17 min in all), and the portability of the newer multicrystal systems are advantages that may outweigh the limitation of a single view.

This study enrolled patients with severe ischemic LV dysfunction and prior myocardial infarction. Since all patients with occluded vessels had angiographically recognized collateral supply to the infarct territory, we cannot exclude the protective effect of preconditioning by recurrent ischemia prior to infarction as a cause of the preserved myocardial viability in 73% of infarcted segments (41,42). Perhaps myocardial viability would be less common following a first myocardial infarction, without antecedent angina or collaterals.

Only 7/43 (16%) biopsies were nonviable. This suggests that patients with prior infarction were chosen for coronary bypass surgery because of evidence for ongoing, active myocardial ischemia (67% had exercise-induced deterioration of regional wall motion on RNA, and 60% gave a history of recent angina). In an effort to collect more nonviable washout data, we are presently studying IPPA washout from segments nonviable by the 3-hr reinjection tomographic thallium technique. To date, we have identified an additional six patients nonviable by reinjection thallium, and the 3-25-min IPPA washout is  $11.3\% \pm 2.6\%$  from the infarcted territories. This compares favorably to the  $13.4\% \pm 2.4\%$  IPPA washout from biopsy nonviable territories.

We realize a more extensive analysis of normal IPPA metabolism, including calculation of elimination rate constants from a larger number of healthy volunteers, is desirable, as is an animal study of infarction utilizing multicrystal IPPA imaging. We, like other investigators (18), noted a large standard deviation of IPPA washout in our healthy volunteers, whereas our patients demonstrated much smaller standard deviations in both the viable and nonviable groups.

However, our criteria for IPPA viability seem sufficient for this study, since IPPA matched biopsy results in 91% of biopsies, and 80% of IPPA viable, revascularized segments demonstrated improved wall motion postoperatively. Our study was designed to evaluate the feasibility

of multicrystal IPPA imaging for viability assessment, and we believe this was accomplished.

## CONCLUSIONS

In contrast to resting wall motion, resting IPPA imaging identifies viable myocardium that otherwise would require another study, such as a reinjection thallium or metabolic PET. Furthermore, viability is usually recognized within 10 min, and always within 17 min. Because of its energy characteristics (159 keV) and 13-hr half-life, IPPA can be imaged with currently available gamma cameras without the necessity of an onsite cyclotron. With the multicrystal technique, as little as 1 mCi of IPPA can be utilized to generate images representing regional rates of beta oxidation. Mobile studies can be performed in the intensive care unit. Imaging of IPPA metabolism sequentially following injection of a short-lived isotope such as iridium could provide a combination wall motion-metabolic study of potential significant clinical value. Therefore, IPPA potentially represents a cost-effective alternative to PET for myocardial viability determination. Further studies, including comparison with PET and reinjection thallium, seem justified.

## ACKNOWLEDGMENTS

The authors thank Norma Dexter for her expertise in processing these studies and Melinda Webb for her diligence in preparing the manuscript.

## REFERENCES

1. Heyndrick GR, Baig H, Nellens P, et al. Depression of regional blood flow and wall thickening after brief coronary occlusions. *Am J Physiol* 1978; 234:H653-H659.
2. Braunwald E, Kloner RA. The stunned myocardium: prolonged, postischemic ventricular dysfunction. *Circulation* 1982;66:1146-1149.
3. Braunwald E, Rutherford JD. Reversible ischemic left ventricular dysfunction: evidence for the "hibernating myocardium." *J Am Coll Cardiol* 1986; 8:1467-1740.
4. Thorn TJ, Kannel WB, Feinleib, M. Factors in the decline of coronary heart disease mortality. In: Connor WE, Briston JD, eds. *Coronary heart disease, prevention, complications, and treatment*. Philadelphia: JB Lippincott; 1985:5-20.
5. Rentrop KP. Thrombolytic therapy in patients with acute myocardial infarction. *Circulation* 1985;71:627-631.
6. Wasserman AG, Ross AM. Patient selection for thrombolytic therapy. *Am J Cardiol* 1989;64:17B-21B.
7. King SB. Patient selection for percutaneous transluminal coronary angioplasty in acute myocardial infarction. *Am J Cardiol* 1989;64:22B-24B.
8. DeWood MA, Heit J, Spores J, et al. Anterior transmural myocardial infarction: effects of surgical coronary reperfusion on global and regional left ventricular function. *J Am Coll Cardiol* 1986;1:1467-1470.
9. DeWood MA, Notske RN, Berg R, et al. Medical and surgical management of early Q-wave myocardial infarction. I. Effects of surgical reperfusion on survival, recurrent myocardial infarction, sudden death, and functional class at 10 or more years of follow-up. *J Am Coll Cardiol* 1989;14:65-77.
10. Lieberman AN, Weiss JL, Judgutt BI, et al. Two-dimensional echocardiography and infarct size: Relationship of regional wall motion and thickening to the extent of myocardial infarction in the dog. *Circulation* 1981;63: 739-746.

11. Schelbert HR. Positron emission tomography: assessment of myocardial blood flow and metabolism. *Circulation* 1985;IV:122-133.
12. Johnston DL, Mulvagh SL, Cashion RW, et al. Nuclear magnetic resonance imaging of acute myocardial infarction within 24 hours of chest pain onset. *Am J Cardiol* 1989;64:172-179.
13. Glueck RM, Mottley JG, Miller JG, et al. Effects of coronary artery occlusion and reperfusion on cardiac cycle-dependent variation of myocardial ultrasonic backscatter. *Circulation Res* 1985;56:683-689.
14. Vered Z, Mohr GA, Bazzilai B, et al. Ultrasound integrated backscatter tissue characterization of remote myocardial infarction in human subjects. *J Am Coll Cardiol* 1989;12:84-91.
15. Kiess M, Lyster D, Belzberg A, et al. I-123 phenylpentadecanoic acid: marker of viability, not just flow [Abstract]. *Circulation* 1987;76:IV-509.
16. Kahn JK, Pippin JJ, Akerr MS, et al. Estimation of jeopardized left ventricular myocardium in symptomatic and silent ischemia as determined by: I-123 phenylpentadecanoic acid rotational tomography. *Am J Cardiol* 1989;63:540-544.
17. Hudon MP, Lyster DM, Jamieson, WR, et al. The metabolism of 15-p-[<sup>123</sup>I]-iodophenylpentadecanoic acid in a surgically induced murine model of regional ischemia. *Eur J Nucl Med* 1990;16:199-204.
18. Kennedy PL, Corbett JR, Kulkarni PV, et al. Iodine 123-phenylpentadecanoic acid myocardial scintigraphy: usefulness in the identification of myocardial ischemia. *Circulation* 1986;74:1007-1015.
19. Hansen CL, Corbett JR, Pippin JJ, et al. Iodine 123-phenylpentadecanoic acid and single photon emission tomography in identifying left ventricular regional metabolic abnormalities in patients with coronary heart disease: comparison with thallium-201 myocardial tomography. *J Am Coll Cardiol* 1988;12:78-87.
20. Vyska K, Machulla HJ, Stemmel W, et al. Regional myocardial free fatty acid extraction in normal and ischemic myocardium. *Circulation* 1988; 78:1218-1233.
21. Schad N, Daue HJ, Ciavolella M, et al. Noninvasive functional imaging of regional rate of myocardial fatty acids metabolism. *Cardiologia* 1987;32: 239-247.
22. Schad V, Wagner RK, Hallermeier J, et al. Regional rates of myocardial fatty acid metabolism: comparison with coronary angiography and ventriculography. *Eur J Nucl Med* 1990;16:205-212.
23. Murray GL, Schad N, Ladd W, et al. Functional cardiac imaging in coronary disease: increased sensitivity of first pass radionuclide angiography utilizing sequential regional left ventricular early diastolic filling rate images. *Cardiologia* 1990;35:25-32.
24. Nickel D, Schad N. Image analysis of the heart action recorded with a high speed multicrystal gamma camera. *Med Progr Technol* 1978;5:1-7.
25. Schad N, Nickel O. Detection of regional flow disturbances with the gamma camera: nuclear imaging of the heart—practical considerations. In: Schaper W, ed. *The pathophysiology of myocardial perfusion*. Amsterdam, New York: Elsevier North Holland, Biomedical Press; 1979:43-61.
26. Schad N. First-pass radiocardiography with the multicrystal gamma camera. In: Diethelm L, Heugh F, Olsson O, Vieten H, Zuppinger A, eds. *Handbuch der medizinischen Radiologie*. Berlin: Springer Verlag; 1985:5-33.
27. Schad N. Nontraumatic assessment of left ventricular wall motion and regional stroke volume after myocardial infarction. *J Nucl Med* 1977;18: 333-341.
28. Liedtke AJ. Alterations of carbohydrate and lipid metabolism in the acutely ischemic heart. *Prog Cardiovasc Dis* 1981;23:321-336.
29. Machulla HJ, Knust EJ, Vyskak. Radioiodinated fatty acids for cardiological diagnosis. *Appl Radiat Isot* 1986;37:777-788.
30. Reske SN, Schon S, Schmitt W, et al. Effect of myocardial perfusion and metabolic interventions on cardiac kinetics of phenylpentadecanoic acid (IPPA) I-123. *Eur J Nucl Med* 1986;12:S27-S31.
31. Antar MA. Radiopharmaceuticals for studying cardiac metabolism. *Nucl Med Biol* 1990;17:103-128.
32. Antar MA. Radiolabeled fatty acids for myocardial studies. In: Spencer RP, ed. *New procedures in nuclear medicine*. Boca Raton, FL: CRC Press; 1989:95-126.
33. Reske SN, Knapp FF, Nitsche J, et al. Preserved I-123 phenylpentadecanoic acid uptake in reperfused myocardium [Abstract]. *J Nucl Med* 1988;29: 842.
34. Reske SN, Knapp FF, Winkler C. Experimental basis of metabolic imaging of the myocardium with radioiodinated aromatic free fatty acids. *Am J Physiol Imag* 1986;1:214-229.
35. Kennedy PL, Wolfe CL, Kulkarni PU, et al. A sensitive means to diagnose myocardial infarction in man: I-123 phenylpentadecanoic acid myocardial imaging [Abstract]. *J Am Coll Cardiol* 1986;7:176A.

36. Morgan CG, Rellas JS, Corbett JR, et al. Quantitative tomographic imaging evaluation of myocardial clearance of I-123 phenylpentadecanoic acid in acute myocardial infarction [Abstract]. *J Am Coll Cardiol* 1983;1:577.
37. Reske SN. I-123-iodophenylpentadecanoic acid as a tracer of cardiac free fatty acid metabolism. Experimental and clinical results. *Eur Heart J* 1985; 6(suppl B):39-47.
38. Schwaiger M, Brunken R, Grover-McKay M, et al. Regional myocardial metabolism in patients with acute myocardial infarction assessed by positron emission tomography. *J Am Coll Cardiol* 1986;8:800-808.
39. Brunken R, Tillisch J, Schwaiger M, et al. Regional perfusion, glucose metabolism, and wall motion in patients with chronic electrocardiographic Q-wave infarctions: evidence for persistence of viable tissue in some infarct regions by positron emission tomography. *Circulation* 1986;73:951-963.
40. Fuster V, Frye RL, Kennedy MA, et al. The role of collateral circulation in the various coronary syndromes. *Circulation* 1979;59:1137-1144.
41. Li GC, Vasquez JA, Gallagher KP, et al. Myocardial protection with preconditioning. *Circulation* 1990;82:609-612.
42. Murry CE, Jennings RB, Reisner KA. Preconditioning with ischemia: a delay of lethal cell injury in ischemic myocardium. *Circulation* 1986;74: 1124-1136.

(continued from page 5A)

## FIRST IMPRESSIONS

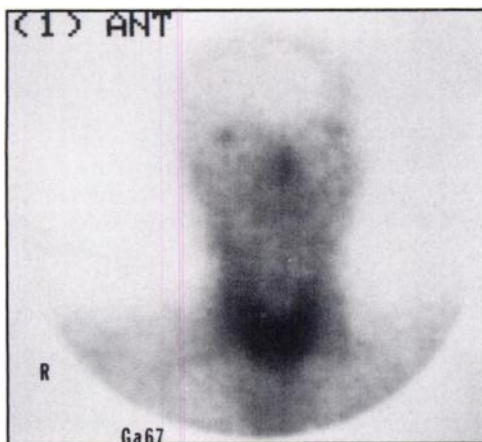


Figure 1

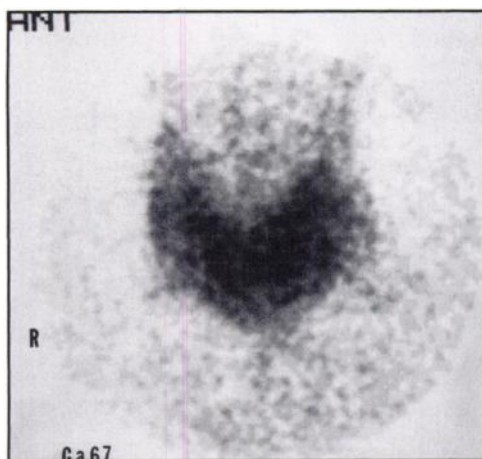


Figure 2

### PURPOSE

A 33-yr-old HIV+ male presented with progressively increasing neck swelling for 2 mo. He was on prophylaxis pentamidine therapy. On physical exam, the thyroid gland was diffusely enlarged and markedly tender to palpation. Iodine-123 uptake was 3.4% at 4 hr and 0.5% at 24 hr. The thin-needle aspiration biopsy of the thyroid at several sites was positive for *Pneumocystis carini* infection and inflammatory exudate. The gallium scan showed intense increased activity throughout the thyroid consistent with *Pneumocystis* thyroiditis. Mild increased activity was also seen in the lungs.

### TRACER

<sup>67</sup>Ga-citrate

### ROUTE OF ADMINISTRATION

Intravenous injection

### TIME AFTER INJECTION

72 hr

### INSTRUMENTATION

General Electric and Picker Gamma Cameras

### CONTRIBUTORS

B. Chandramouly, MD

### INSTITUTION

Long Island College Hospital, Brooklyn NY